IIETA International Information and Engineering Technology Association
Advancing the World of Information and Engineering

Instrumentation Mesure Métrologie
Vol. 24, No. 5, October, 2025, pp. 325-334
Journal homepage: http://iieta.org/journals/i2m

Investigation of Temperature Parameters in PETG Additive Printing

Miroslav H. Hristov[1], Kliment K. Georgiev[2*]

[1] Department of Energy and Mechanical Engineering, Technical College – Sofia, Technical University of Sofia, Sofia 1000, Bulgaria
[2] Department of Instrumentation and Mechanical Engineering, Technical University of Sofia, Plovdiv 4000, Bulgaria

Corresponding Author Email: k.georgiev@tu-plovdiv.bg

https://doi.org/10.18280/i2m.240504

Received: 11 September 2025
Revised: 13 October 2025
Accepted: 23 October 2025
Available online: 31 October 2025

Keywords:
additive manufacturing, design of experiment, quality control, coordinate measuring machine, measurements, optimal parameters

ABSTRACT

Technological advancements over the past few decades have had a profound impact on the field of additive printing technologies. Additive printing technologies are becoming increasingly important in the manufacturing sector, where they are employed for the rapid and cost-effective production of prototypes. The present article examines the influence of the nozzle temperature and the printer bed temperature. A meticulously planned experiment methodology is employed, with three series of experiments conducted to ascertain the optimal printing parameters. A thorough examination of the results yielded from the meticulously designed experiments has determined that the optimal nozzle temperature is 245°C, while the optimal bed temperature is 85°C. Regression equations are derived. The values obtained for the controlled dimensions are outside the prescribed tolerances. This necessitates further research to determine the shrinkage coefficient of the material used.

1. INTRODUCTION

Additive manufacturing (AM) is the primary choice for generating a hierarchical product directly from a computer-aided design (CAD) file. AM is a widely used technology for advanced 3D design and is also known as 3D printing [1]. The physical principle of AM dates back to the end of the 19th century, when it was developed in the context of two distinct applications that are now considered to be the precursors of AM: photosculpture and topography [2]. The development and widespread use of AM methods such as 3D printing in recent years can be attributed to their adaptability, speed of reaction and low cost. This technology has benefited many sectors, including construction, medicine, robotics, the military, automotive and aerospace, to name a few. Moreover, AM offers benefits such as reduced manufacturing costs and the ability to tailor low-volume items to individual customers' preferences in a cost-effective and expedited manner. Thanks to applications of the AM process, less expensive materials, moulds, and dies may be used. This method enables businesses or individuals to save money while experimenting with new ideas [3].

Fused deposition modeling (FDM) using polyethylene terephthalate glycol-modified (PETG) filament is widely employed for its strength, flexibility, and ease of printing relative to other thermoplastics. However, PETG presents unique challenges, including stringing, inconsistent bridging, and thermal expansion effects, which must be managed through precise process parameter tuning. Among these parameters, nozzle and bed temperature settings are critical in determining both the dimensional accuracy and surface quality of printed parts. The Prusa MK4, a printer with enhanced firmware and thermal management capabilities, introduces additional considerations regarding cooling dynamics and extrusion stability. Despite the importance of optimizing nozzle and bed temperatures for PETG, existing literature fails to specifically address these interactions within the context of the Prusa MK4.

Recent experimental studies have explored factors influencing PETG print quality, with emphases on either dimensional accuracy or surface roughness outcomes. Several works apply optimization frameworks such as the Taguchi method [4-7], response surface methodology (RSM) [8, 9], and Bayesian optimization [10] to identify parameter settings for PETG printing. Studies consistently report that nozzle temperature impacts dimensional accuracy and layer adhesion, with optimal temperatures identified between 230°C and 250°C [4, 6-8]. However, bed temperature effects remain less studied, with most research fixing this parameter (e.g., at 70°C or 80°C) rather than investigating its interaction with nozzle temperature [5, 8, 11]. One exception is the research [9], which found that bed temperature contributed 39.7% to dimensional variability, suggesting it plays a more significant role than previously assumed.

Surface quality studies have primarily examined nozzle temperature, fan speeds, and layer height [10-12]. Lower nozzle temperatures between 220°C-230°C have been associated with reduced surface roughness but weaker interlayer bonding, whereas temperatures above 240°C risk increased stringing [11, 12]. However, these findings remain printer-agnostic, with test conditions based on machines such as the Creality Ender 3 V2 [11] or Prusa i3MK3S+ [10],

leaving gaps in their applicability to the Prusa MK4's upgraded dual-fan cooling and uniform heating system. Additionally, none of the available studies consider the Prusa MK4's firmware features, such as input shaping and pressure equalization, which influence extrusion consistency.

While existing research provides valuable insights into nozzle temperature selection and dimensional accuracy trends for PETG printing, critical gaps remain regarding the explicit interaction between nozzle and bed temperature settings, optimization tailored to the Prusa MK4's hardware-specific characteristics, and integrated evaluations of both dimensional accuracy and surface quality. Given the MK4's unique thermal and motion control capabilities, further research is needed to systematically analyze temperature interactions and establish optimized settings for PETG printing on this platform.

Polyethylene terephthalate glycol (PETG) is a popular filament for FDM thanks to its toughness, chemical resistance and relatively low warpage compared to ABS. However, its dimensional behaviour is governed by complex interactions between thermal history, viscoelastic relaxation, bead formation and machine/slicer settings. This review synthesises a generic systematic review of FDM process parameters and dimensional accuracy, and the currently scattered body of PETG-specific experimental studies on dimensional deviation and geometric fidelity. No PETG-focused review of dimensional accuracy exists. Available studies show that layer height and build plate temperature are the most influential parameters for PETG dimensional accuracy, while nozzle temperature, printing speed and infill/shell structure play important, albeit secondary, roles. Most PETG studies quantify global linear deviations or feature-level diameter/height errors, with very limited data on warpage, shrinkage curves, build orientation, cooling or time-dependent dimensional drift [4, 8, 9, 13].

The objective of the present report is to conduct a thorough investigation into the optimal operating temperatures for additive printing and PETG material. The experimental methodology employed in this study was of a classic, planned nature, with the objective of evaluating the results obtained. The requisite single-factor experiments were conducted, subsequently followed by a two-factor experiment. The results obtained are presented in tabular form and subsequently analysed.

2. MATERIALS AND METHODS

2.1 Printed detail

The "bushing" detail shown in Figure 1 is selected for conducting the experiments.

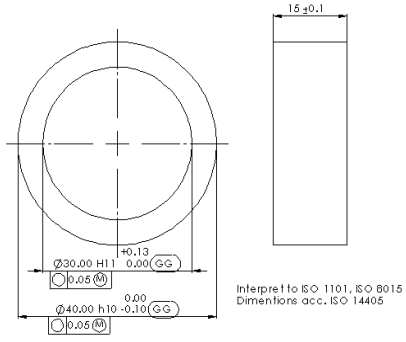

Figure 1. Test part drawing

2.2 Used material

The test details are made of Polyethylene Terephthalate Glycol (PETG), PETG material exhibits low shrinkage upon heating, high tensile strength, and exceptional layer adhesion properties, rendering it a highly versatile material in various industrial and scientific applications [14]. Polyethylene terephthalate (PET) is a polyester copolymer that boasts a number of advantageous technical specifications, including durability, flexibility, high impact resistance, high chemical resistance, and low moisture absorption, amongst others [15]. The technical specifications of the material selected are enumerated in Tables 1 and 2.

Table 1. Technical specification of PETG [16]

Chemical Name	Polyethylene Terephthalate Glycol Copolymer
Melting temperature	210 - 260°C
Working temperature (3D printer)	250 ± 10°C
Print bed temperature	80 ± 10°C
Print speed	up to 200 mm/s
Moisture absorption in 24 hours	0.07%
Moisture absorption in 7 days	0.10%
Heat deflection temperature (0.45 MPa)	68°C
Heat deflection temperature (1.80 MPa)	68°C

Table 2. Mechanical properties of PETG [16]

Property/ Print Direction	Horizontal	Vertical xz
Tensile yield strength [MPa]	47 ± 2	50 ± 1
Tensile modulus [GPa]	1.5 ± 0.1	1.6 ± 0.1
Elongation at yield point [%]	5.1 ± 0.1	5.1 ± 0.1
Flexural strength [MPa]	66 ± 2	70 ± 1
Flexural modulus [GPa]	1.7 ± 0.1	1.6 ± 0.1
Deflection at flexural strength [mm]	9.0 ± 0.1	9.3 ± 0.2
Impact strength charpy [kJ/m^2]	No break	No break
Impact strength charpy notched [kJ/m^2]	6 ± 1	3 ± 1

2.3 Additive manufacturing technology

The ISO / ASTM 52900 [17] standard categorizes all the different types of 3D printing. The 3D printing technology chosen is FDM as shown in Figure 2. It is an additive manufacturing method where layers of materials are fused together in a pattern to create an object. FDM is the most cost-effective way to produce custom thermoplastic parts and prototypes.

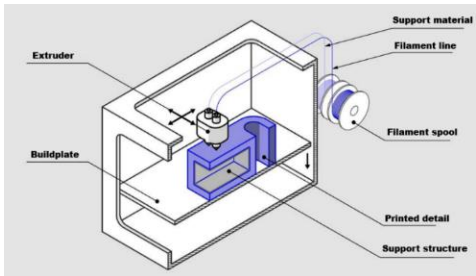

Figure 2. Schematic diagram of FDM technology [18]

A plethora of thermoplastic materials is available for FDM, rendering them suitable for both prototyping and certain functional applications [19].

A key limitation of FDM is its comparatively poor dimensional accuracy and resolution when compared to other 3D printing technologies. The presence of visible lines on FDM parts necessitates subsequent treatment for smooth surfaces. Furthermore, the adhesion mechanism of the layer renders FDM particles inherently anisotropic. This inherent anisotropy renders the particles weaker in one direction, thus rendering them unsuitable for critical applications.

2.4 3D printer used

A Prusa MK4 printer is used to produce the test details Figure 3. The characteristics of the printer used are listed in Table 3. The MK4 printer is the fourth generation of FMD printer from PRUSA Research, offering reliability, high quality and repeatability of finished parts. The utilisation of stepper motors with a step angle of 0.9° ensures the production of components of a higher quality.

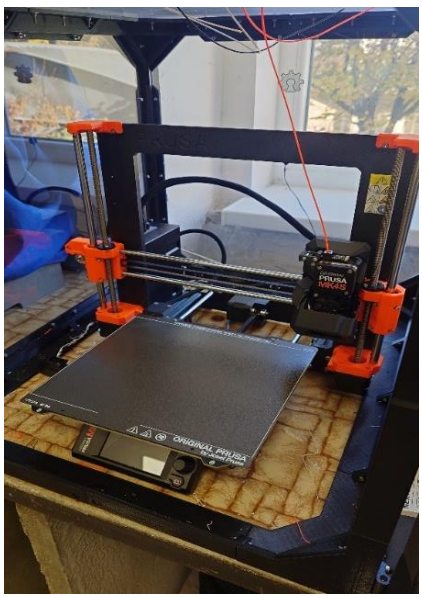

Figure 3. Prusa Mk4s

Table 3. Technical specification of Prusa MK4 [20]

Technical Parameters	
Build volume	250 × 210 × 220 mm
Filament diameter	1.75 mm
Layer height	0.05-0.30 mm
Stepper motors	Precise 0.9° X, Y stepper motors
Max nozzle temperature	290°C
Max heatbed temperature	120°C
Supported materials	PLA, PETG, Flex, PVA, PC, PP, CPE, PVB

2.5 Measuring system

To evaluate the results obtained from FDM using PETG filament, we use a CMM Aberlink Horizon. The machine has a bridge design and uses linear motors for more precise positioning and higher speed to achieve MPEE = 1.5 µm + L/350 mm [21], optical scales Renishaw with resolution 0.1 µm are used and probe head Renishaw SP25M [22].

2.6 Design of experiment

Experimental design is a foundational component of empirical research, providing structured methodologies for investigating causal relationships while minimizing confounding and maximizing efficiency. Central to this domain are single-factor, two-factor, and factorial experimental designs, each offering progressively richer frameworks for evaluating main effects and interactions. The corpus of literature identified in this review emphasizes the theoretical underpinnings and methodological strategies associated with these designs, ranging from fundamental principles to advanced statistical innovations.

A substantial portion of the literature focuses on establishing the core principles essential to any experimental framework—randomization, replication, and blocking. Foundational texts such as Ireland's fundamental concepts in the design of experiment [23] and Wu and Hamada's experiments [24] provide comprehensive treatments of these concepts, detailing their implementation in single-factor and multi-factor settings. These works are complemented by broader resources such as Bowerman's statistical design and analysis of experiments [25], which integrates inferential tools like ANOVA with design considerations for both fixed and random effects.

Several references explore factorial designs in depth, offering theoretical and practical guidance on structuring experiments with multiple independent variables and interpreting interaction effects. Collins et al. [26] address the trade-offs between complete and fractional factorial designs, discussing power considerations, aliasing, and resource constraints. Their work is extended by Dziak et al. [27], who provide detailed guidance on factorial design strategies for behavioral science applications, including multilevel and clustered factorial structures.

Fractional factorial designs—used to reduce the number of conditions in multi-factor experiments—receive focused attention in multiple sources. Gunst and Mason [28] summarize key statistical properties and design strategies, while Hoshmand [29] and Voelkel [30] provide practical examples and techniques for constructing and analyzing such designs, including the implications of resolution and confounding. Bayesian approaches to fractional factorial design are explored by Toman [31], who derives Bayes-optimal designs in two- and three-level settings, highlighting the method's utility in sparse-data conditions.

Advanced methodologies such as response surface methodology (RSM) and split-plot designs are also represented. Chandra et al. [32] and Ryan [33] include RSM applications for continuous factor levels and process optimization, while Zhao [34] discusses clear-effect criteria in fractional factorial split-plot (FFSP) designs where randomization constraints exist between whole-plot and subplot factors.

Finally, domain-specific adaptations illustrate how these principles are applied and extended. Hoshmand [29] details the use of single- and multi-factor designs in agricultural research, while Singh and Chauhan [35] focus on factorial optimization frameworks in pharmaceutical contexts. Across these applications, the link between statistical methodology and experimental structure remains a central concern.

Together, these references provide a detailed and

methodologically rich landscape of theoretical and practical contributions to the design and analysis of single-factor, two-factor, and factorial experiments. Through this literature, key elements such as interaction analysis, efficient resource allocation, and statistical rigor are shown to be deeply interwoven in both foundational theory and evolving experimental practice.

Regression analysis is a compulsory component of the DoE application, as it facilitates the modelling and investigation of the relationship between linear dimensions and bed/nozzle temperatures in FDM. The primary function of the generated mathematical model is to provide a framework for analysing the relationship between the variables under investigation, thereby facilitating a comprehensive examination of the resultant data. A key application of this methodology is linear approximation, most often through the least squares approach (OLS). This provides further insight into the proximity of the obtained mathematical model to the experimental results under consideration. The linear regression equation is the main tool of regression analysis [36]:

$$D(S) = a.t^1 + b.t^0 \quad (1)$$

where, D – controlled diameter, t – test temperature, S – sequence of the test series.

3. RESULTS AND DISCUSSION

The present study investigates the influence of the nozzle temperature and the printer bed temperature on the geometric accuracy of the part. The measurement of the test samples is performed with a CMM Aberlink Horizon [22] (Figure 4), which controls the cylinder measured in three sections and calculated according to GD&T principles and ISO 14405 [37] – using the least squares method (GG), minimum described element (GX), and maximum inscribed element (GN). To comparison, the test samples are also measured as a circle designed in a plane located in the middle of the sample. The tabulated results (Tables 4, 5, and 6) correspond to the measured cylinder values.

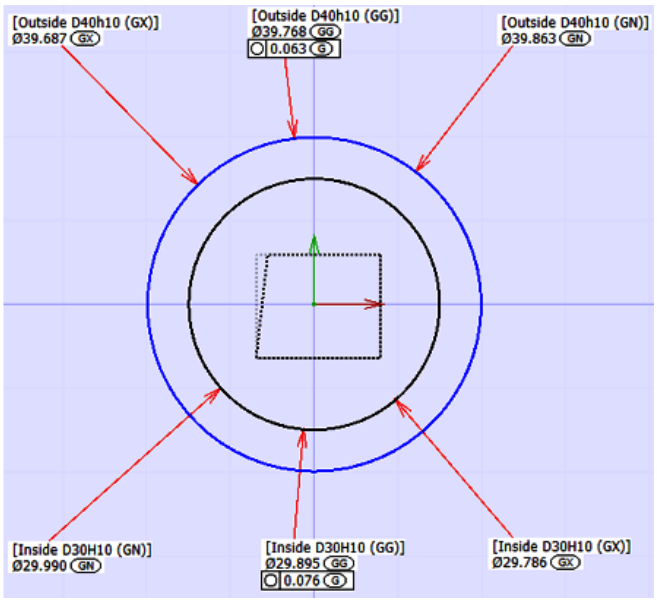

Figure 4. Visualization of sample measurement results with CMM Aberlink Horizon [22, 38]

Single-factor experiments were conducted for the selected technological parameters, and the influence of each of them was investigated. Following the determination of the optimal values, a two-factor experiment was conducted to establish the combination of temperatures that yielded the best results. The measured dimensions are defined as the outer and inner diameters of the component illustrated in Figure 1. In consideration of the experience garnered in preceding experiments, no substantial fluctuations in the specified parameter were observed. Consequently, no experimental data pertaining to this parameter is presented in this study. The experiments were conducted in three series. The results for each series are presented in two tables. It is imperative to undertake this presentation because the outer and inner diameters have been measured. The data pertaining to the mean diameter of all series is presented graphically.

$$Din = f(t_b[°C], t_n[°C]) \quad (2)$$

where, Din - inner diameter of the controlled samples, t_b - printer bed temperature, t_n - nozzle temperature.

$$\Delta Din = Din(n) - Din(GG) \quad (3)$$

where, ΔDin – relative change in internal diameter of the controlled samples, Din(n) – nominal value of inner diameter, Din(GG) inner diameter value obtained by the least squares method [29].

$$Dout = f(t_b[°C], t_n[°C]) \quad (4)$$

where, Dout – outer diameter of the controlled samples.

$$\Delta Dout = Dout(n) - Dout(GG) \quad (5)$$

where, ΔDout – relative change in the outer diameter of the controlled samples, Dout(n) – nominal value of outer diameter, Dout(GG) – outer diameter value obtained by the least squares method [37].

Series 1 - single-factor experiment to determine the optimal nozzle temperature. After analyzing the PETG offered on the market by different manufacturers, the limits of the experiment and the step were determined. For this material, a research range of 220 to 265°C and a step of 5°C were determined. The results are presented in Table 4.

$$\Delta t_n = t_{n(k+1)} - t_{n(k)} = 5°C \quad (6)$$

where, Δt_n – change in nozzle temperature, k – serial number of the test at a step of 5°C.

$$\Delta t_b = t_{b(j+1)} - t_{b(j)} = 5°C \quad (7)$$

where, Δt_b – change in bed temperature, j – sequential number of the experiment in step 5°C.

Based on the experiments conducted and the results obtained from Series S1, we obtain the following regression equations:

$$y(S1.1) = 0.0089x + 0.2222 \quad (8)$$

$$y(S1.2) = -0.0046x + 0.1389 \quad (9)$$

Table 4. Series 1 results (designations GG, GX, GN – definition according to ISO 14405 [37])

k	t_n, [°C]	S 1.1 - Outer Diameter (Dout), [mm], Bed Temp (t_b) =const = 85 [°C]				S 1.2 - Inner Diameter (Din), [mm], Bed Temp (t_b) = const = [85°C]			
		Dout (GX)	Dout (GN)	Dout (GG)	ΔDout	Din (GX)	Din (GN)	Din (GG)	ΔDin
1	220	39.716	39.883	39.797	0.203	29.711	29.926	29.844	0.156
2	225	39.674	39.852	39.759	0.241	29.743	29.948	29.875	0.126
3	230	39.621	39.813	39.71	0.29	29.808	29.977	29.904	0.096
4	235	39.651	39.818	39.735	0.265	29.768	29.984	29.891	0.109
5	240	39.65	39.808	39.73	0.270	29.767	29.96	29.888	0.112
6	245	39.635	39.829	39.735	0.265	29.755	29.923	29.848	0.152
7	250	39.651	39.841	39.744	0.256	29.756	29.971	29.888	0.112
8	255	39.627	39.801	39.708	0.292	29.795	30.022	29.908	0.092
9	260	39.58	39.801	39.677	0.323	29.812	30.005	29.929	0.071
10	265	39.574	39.831	39.696	0.304	29.735	29.984	29.89	0.110

Table 5. Series 2 results (GG, GX, GN – acc. ISO 14405 [37])

k	t_b, [°C]	S 2.1 - Outer Diameter (Dout), [mm], nozzle temp (t_n) = const = 245 [°C]				S 2.2 - Inner Diameter (Din), [mm], Nozzle Temp (t_n) = const = 245 [°C]			
		Dout (GX)	Dout (GN)	Dout (GG)	ΔDout	Din (GX)	Din (GN)	Din (GG)	ΔDin
1	55	39.603	39.776	39.68	0.320	29.838	30.024	29.951	0.049
2	60	39.583	39.821	39.713	0.287	29.795	30.024	29.917	0.083
3	65	39.545	39.821	39.664	0.336	29.805	30.106	30.010	-0.010
4	70	39.687	39.863	39.768	0.232	29.786	29.990	29.895	0.105
5	75	39.604	39.807	39.707	0.293	29.803	30.007	29.927	0.073
6	80	39.613	39.786	39.694	0.306	29.796	29.987	29.905	0.095
7	85	39.668	39.841	39.750	0.250	29.751	29.929	29.845	0.155
8	90	39.657	39.806	39.718	0.282	29.742	29.916	29.842	0.158
9	95	39.564	39.719	39.637	0.363	29.783	29.981	29.902	0.980
10	100	39.587	39.776	39.685	0.315	29.803	30.012	29.925	0.075

Table 6. Series 3 results (GG, GX, GN – acc. ISO 14405 [37])

n	t_b/t_n, [°C]	S 3.1 - Outer Diameter (Dout), [mm]				S 3.2 - Inner Diameter (Din), [mm]			
		Dout (GX)	Dout (GN)	Dout (GG)	ΔDout	Din (GX)	Din (GN)	Din (GG)	ΔDin
1	245/85	39.635	39.829	39.735	0.265	29.755	29.923	29.848	0.152
2	245/90	39.657	39.806	39.718	0.280	29.742	29.916	29.842	0.158
3	245/80	39.613	39.786	39.694	0.306	29.796	29.987	29.905	0.095
4	240/80	39.616	39.774	39.686	0.314	29.928	29.987	29.934	0.066
5	240/85	39.650	39.808	39.730	0.270	29.767	29.960	29.888	0.112
6	240/90	39.644	39.802	39.719	0.281	29.943	29.773	29.872	0.128
7	250/80	39.607	39.734	39.675	0.325	29.812	30.051	29.945	0.055
8	250/85	39.651	39.841	39.744	0.265	29.756	29.971	29.888	0.112
9	250/90	39.601	39.756	39.680	0.320	29.758	29.947	29.872	0.128

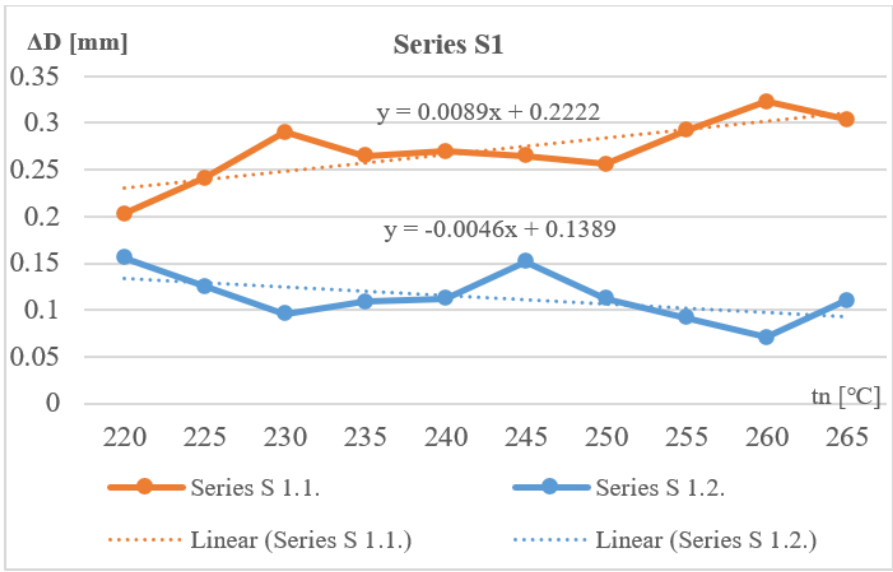

Figure 5. Trendline (Series S1.1, S1.2) and linear regression model of Din and Dout related to nominal size D(n) as a function of temperature (t_n)

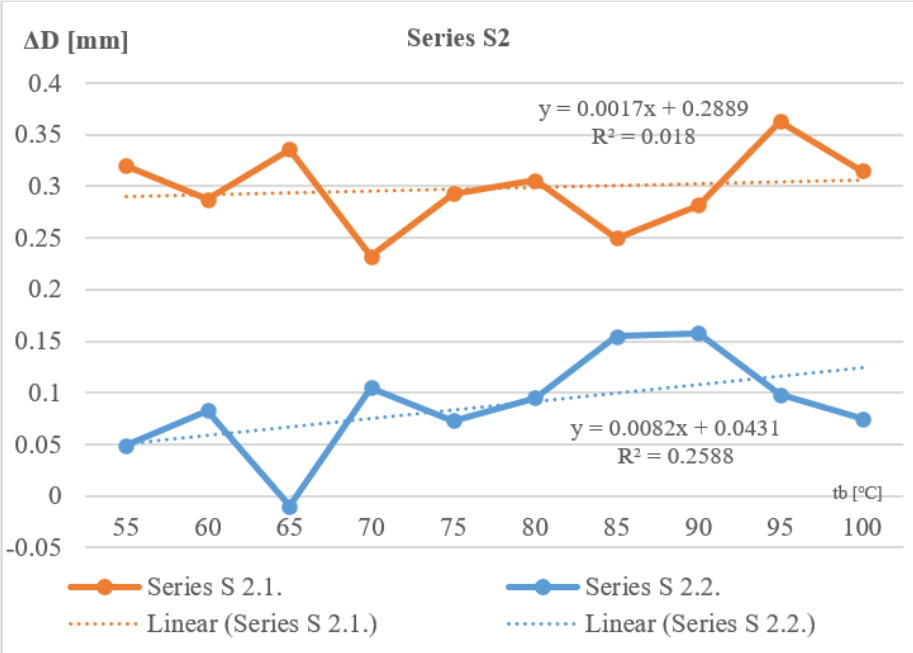

Figure 6. Trendline (Series S2.1, S2.2) and linear regression model of Din and Dout related to nominal size D(n) as a function of temperature(t_n)

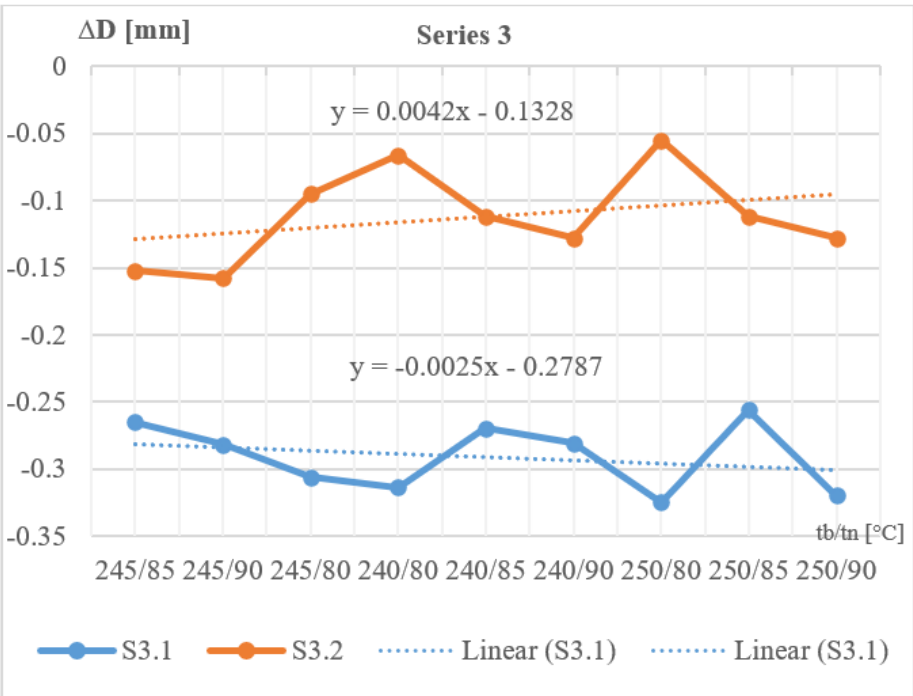

Figure 7. Trendline (Series S3.1, S3.2) and linear regression model of Din and Dout related to nominal size D(n) as a function of temperature(t_n)

The measurement results show that at a nozzle temperature of 220°C, the results are closest to the nominal rammer, and at values between 240 and 250°C, relatively similar results are obtained. Figure 5 shows the average values of the measured dimensions.

In terms of internal dimensions, the best results are achieved at 260°C, with results at temperatures between 240 and 250°C being relatively similar. The results for temperatures below 230°C and above 255°C are outside the recommended PETG printing values and can be considered gross errors. During the experiments for series 2, a nozzle temperature of 245°C was selected, as some of the best results were obtained at this temperature, and the value is within the recommended upper limits for the material.

Series 2 – determining the optimum table temperature. Once again, an analysis of the market for similar materials was carried out and the scope of the experiment and the steps were determined as follows: table temperature from 55 to 100°C and steps of 5°C. Table 5 shows the results obtained from the measurements for the outer and inner diameters.

Based on the experiments conducted and the results obtained from Series S2(Figure 6), we obtain the following

regression equations:

$$y(S2.1) = 0.0017x+0.2889 \quad (10)$$

$$y(S2.2) = 0.0082x+0.0431 \quad (11)$$

The regression equations presented for series S1.1 and S1.2 show the change in the results obtained for the different test details. The coefficients of the equations for internal dimensions are significantly lower than those for external dimensions, which is consistent with the experimental data obtained. For the external diameter, a higher coefficient of dimensional shrinkage relative to the nominal dimensions is observed.

At table temperatures between 55°C and 75°C, weaker adhesion is observed, which can lead to destruction of the part. At temperatures above 90°C, changes in the quality of the layers are observed. For these reasons, a nozzle temperature of 245°C and a mass temperature of 85°C were selected as the zero level for the experiments in series 3(Figure 7). The results obtained from the first two series show that all measurements are outside the specified tolerances, with shrinkage of the materials observed, which is different for the outer and inner diameters. However, the results are similar, which allows us to continue with the tests in series 3. In order to achieve the specified tolerances, it is necessary to examine the expansion and shrinkage of the specific material and to correct the 3D model in order to achieve the initially specified dimensions.

Series 3 – Two-factor experiment. After analyzing the single-factor experiments, the optimal values of the nozzle and mass were determined to be 245/85°C. The values of the other temperatures were determined relative to the selected zero level. A single-factor experiment with levels ±1 from zero was selected, using a step of 5°C for both factors. The results are presented in Table 6.

Based on the experiments conducted and the results obtained from Series S3, we obtain the following regression equations:

$$y(S3.1) = -0.0025-0.2787 \quad (12)$$

$$y(S3.2) = 0.0042x-0.1328 \quad (13)$$

The obtained regression equations show closer results for coefficients due to the optimization of temperatures t_n and t_b. The results obtained thus enable us to develop a methodology for accounting for and compensating for the relative error εδ in printing as a ratio of the change in diameters to the nominal value:

$$\varepsilon_\delta[\mu m/mm] = \frac{\Delta D[mm]}{D(n)[mm]}.1000 \quad (14)$$

where, εδ - relative error in μm/mm, ΔD - relative change in diameter of the controlled samples, D(n) - nominal diameter.

Presenting the relative error εδ in Table 7 and Figure 8 as a value in μm/mm enables direct correction of the printed dimensions.

Table 7. Relative error εδ in μm/mm

Series	S 1.1 (Dout)		S 1.2 (Din)		S 2.1 (Dout)		S 2.2 (Din)		S 3.1 (Dout)		S 3.2 (Din)	
k = j = n	ΔDout [mm]	εδout [μm]	ΔDin [mm]	εδin [μm]	ΔDout [mm]	εδout [μm]	ΔDin [mm]	εδin [μm]	ΔDout [mm]	εδout [μm]	ΔDin [mm]	εδin [μm]
1	0.203	5.075	0.156	5.200	0.320	8.000	0.049	1.633	0.265	6.625	0.152	5.067
2	0.241	6.025	0.126	4.200	0.287	7.175	0.083	2.767	0.280	7.000	0.158	5.267
3	0.290	7.250	0.096	3.200	0.336	8.400	-0.010	3.333	0.306	7.650	0.095	3.167
4	0.265	6.625	0.109	3.633	0.232	5.800	0.105	3.500	0.314	7.850	0.066	2.200
5	0.270	6.750	0.112	3.733	0.293	7.325	0.073	2.433	0.270	6.750	0.112	3.733
6	0.265	6.625	0.152	5.067	0.306	7.650	0.095	3.167	0.281	7.025	0.128	4.267
7	0.256	6.400	0.112	3.733	0.250	6.250	0.155	5.167	0.325	8.125	0.055	1.833
8	0.292	7.300	0.092	3.067	0.282	7.050	0.158	5.267	0.265	6.625	0.112	3.733
9	0.323	8.075	0.071	2.367	0.363	9.075	0.098	3.267	0.320	8.000	0.128	4.267

* εδin and εδout - relative error of the change in ΔD divided of the nominal diameter D(n)

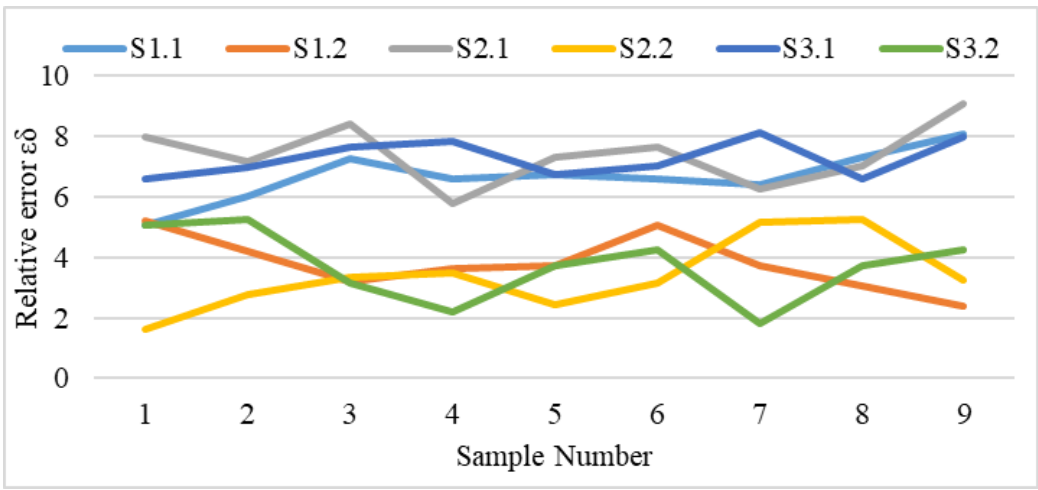

Figure 8. Relative error εδ distribution chart

The results obtained were used to derive the relative regression equations (y(εδin) and y(εδout)) from the data presented in Table 7 and Figure 8 for the three series S1, S2, and S3.

$$y(\varepsilon\delta in) = -00181x+3.7302 \quad (15)$$

$$y(\varepsilon\delta out) = 0.1117x+6.5713 \quad (16)$$

We have two linear regression equations that express the linear dependence of the error εδ as a function of the change in the temperature ratio t_b/t_n.

An essential factor for optimizing the geometric dimensions relative to the change in temperatures t_b and t_n is finding the closest points from the graphs (equations) in the recommended conditions for printing the selected material.

The results obtained show that several temperature combinations have very similar values for the controlled parameters. Each of the samples exhibits good adhesion to the printer bed, with so-called "stringing" occurring at temperatures above 245℃. Comparing the results for the two controlled dimensions, 245/85℃ was selected as the optimal temperature. At this temperature, a balance was observed between the measured dimensions, and the values were within the limits recommended by the filament manufacturers.

4. CONCLUSIONS

The article presents a study of the optimal printing parameters for PETG using FDM. The determination of the optimal printing parameters for the nozzle and printer table was achieved through the implementation of a design of experiment methodology. The experimental results are validated through two-factor experiments. Following a comprehensive analysis of the results obtained, it was determined that the optimal combination for the temperature of the nozzle and printer table was 245/85℃. It has been determined that none of the controlled parameters meet the tolerance set for the part. This is due to the fact that all of the geometric parameters are out of tolerance limits. It is therefore necessary to adjust the nominal dimensions in the 3D model to achieve the specified tolerances. It is evident from the research that has been conducted and the regression equations that have been determined that there is the possibility of selecting random parameters for the selection of the temperature for the nozzle and printer table. In this context, linear compensation should be introduced. The developed mathematical models can serve as an applied methodology for optimising the geometric dimensions of printed parts by additive printing for both PETG material and materials with common printing temperature characteristics.

ACKNOWLEDGMENT

The authors would like to thank the Research and Development Sector at the Technical University of Sofia for the financial support.

REFERENCES

[1] Dawood, J.J., Ali, H.B., Anaee, R., Mohammed, F.M. (2025). Characterizing and optimizing the parameters of additive manufacturing by fused deposition modeling methods to enhance the product mechanical qualities. International Journal of Computational Methods and Experimental Measurements, 13(1): 133-140. https://doi.org/10.18280/ijcmem.130114

[2] Salem, H., Abouchadi, H., El Bikri, K. (2025). A design methodology for additive manufacturing-fused deposition modeling case study. International Journal of Computational Methods and Experimental Measurements, 13(2): 449-463. https://doi.org/10.18280/ijcmem.130220

[3] Taresh, O.F., Mezher, M.T., Daway, E.G. (2023). Mechanical properties of 3D-printed PETG samples: The effect of varying infill patterns. Revue des Composites et des Matériaux Avancés, 33(5): 339-345. https://doi.org/10.18280/rcma.330508

[4] Muhammad, A.R., Sakura, R.R., Dwilaksana, D., Sumarji, Trifiananto, M. (2022). Layer height, temperature nozzle, infill geometry and printing speed effect on accuracy 3D printing PETG. Rekayasa Energi Manufaktur Jurnal, 7(2): 81-88. https://doi.org/10.21070/r.e.m.v7i2.1649

[5] Rosa, R., Subhan, M., Pristiansyah, P. (2024). Pengaruh parameter proses pada pencetakan 3D printing terhadap akurasi dimensi filamen petg menggunakan metode taguchi. Jurnal Inovasi Teknologi Terapan, 2(1): 79-87. https://doi.org/10.33504/jitt.v2i1.149

[6] Zulfitriyanto, Z., Putri, S.F., Pristiansyah, P. (2025). Pengaruh nozzle temperature dan layer height terhadap akurasi dimensi produk ulir menggunakan filamen PETG. Jurnal Inovasi Teknologi Terapan, 3(1): 250-256. https://doi.org/10.33504/jitt.v3i1.320.

[7] Wahyudi, W., Suzen, Z.S., Pristiansyah, P. (2025). Pengaruh parameter proses pencetakan 3D printing terhadap kebulatan produk menggunakan filament PETG. Jurnal Inovasi Teknologi Terapan, 3(1): 207-213. https://doi.org/10.33504/jitt.v3i1.305

[8] Mishra, P., Sood, S., Bharadwaj, V., Aggarwal, A., Khanna, P. (2023). Parametric modeling and optimization of dimensional error and surface roughness of fused deposition modeling printed polyethylene terephthalate glycol parts. Polymers, 15(3): 546. https://doi.org/10.3390/polym15030546

[9] Abdulridha, H.H., Obaeed, N.H., Jaber, A.S. (2025). Optimization of fused deposition modeling parameters for polyethylene terephthalate glycol flexural strength and dimensional accuracy. Advances in Science and Technology Research Journal, 19(4): 50-64. https://doi.org/10.12913/22998624/200088

[10] Kolte, A., Bhaskaran, V., Hoyle, C. (2024). Optimizing 3D printing process parameters to minimize surface roughness using bayesian optimization. In Volume 2A: 44th Computers and Information in Engineering Conference (CIE). American Society of Mechanical Engineers. https://doi.org/10.1115/detc2024-143297

[11] Taqdissillah, D., Muttaqin, A.Z., Darsin, M., Dwilaksana, D., Ilminnafik, N. (2022). The effect of nozzle temperature, infill geometry, layer height and fan speed on roughness surface in PETG filament. Journal of Mechanical Engineering Science and Technology, 6(2): 74. https://doi.org/10.17977/um016v6i22022p074

[12] Aji, B., Pristiansyah, P., Ariyani, Y.F. (2023). Pengaruh parameter proses terhadap kekasaran permukaan

menggunakan filamen PETG (Polyethylene terephthalate glycol). Jurnal Inovasi Teknologi Terapan, 1(2): 332-338. https://doi.org/10.33504/jitt.v1i2.32
[13] Natarajan, M., Pasupuleti, T., Kiruthika, J., D, P., Silambarasan, R. (2024). Optimization and regression modeling of additive manufacturing (Fused deposition modeling) of PETG material for automobile applications. In SAE Technical Paper 2024-28-0234. https://doi.org/10.4271/2024-28-0234
[14] Durgashyam, K., Indra Reddy, M., Balakrishna, A., Satyanarayana, K. (2019). Experimental investigation on mechanical properties of PETG material processed by fused deposition modeling method. Materials Today: Proceedings, 18: 2052-2059. https://doi.org/10.1016/j.matpr.2019.06.082
[15] Valvez, S., Silva, A.P., Reis, P.N.B. (2022). Optimization of printing parameters to maximize the mechanical properties of 3D-printed PETG-based parts. Polymers, 14(13): 2564. https://doi.org/10.3390/polym14132564
[16] Prusament PETG Jet Black 2kg. https://www.prusa3d.com/product/prusament-petg-jet-black-2kg/.
[17] ASTM International. (2015). ISO/ASTM 52900: Additive manufacturing — General principles — Terminology. https://www.astm.org/Standards/ISOASTM52900.htm.
[18] What is FDM (fused deposition modeling) 3D printing? https://www.hubs.com/knowledge-base/what-is-fdm-3d-printing/.
[19] Dudek, P. (2013). FDM 3D printing technology in manufacturing composite elements. Archives of Metallurgy and Materials, 58(4): 1415-1418. https://doi.org/10.2478/amm-2013-0186
[20] Original Prusa MK4S 3D Printer. https://www.prusa3d.com/product/original-prusa-mk4s-3d-printer-5/#specs.
[21] ISO 10360-7:2011. Geometrical product specifications (GPS) — Acceptance and reverification tests for coordinate measuring machines (CMM). https://www.iso.org/standard/43904.html.
[22] Horizon CMM. https://www.aberlink.com/products/coordinate-measuring-machines/horizon/.
[23] Ireland, C. (1965). Fundamental concepts in the design of experiments. Technometrics, 7(4): 652-653. https://doi.org/10.1080/00401706.1965.10490308
[24] Wu, C.J., Hamada, M.S. (2011). Experiments: Planning, Analysis, and Optimization. John Wiley & Sons.
[25] Bowerman, B.L. (1991). Statistical design and analysis of experiments with applications to engineering and science. Technometrics, 33(1): 105-106. https://doi.org/10.1080/00401706.1991.10484774
[26] Collins, L.M., Dziak, J.J., Li, R. (2009). Design of experiments with multiple independent variables: A resource management perspective on complete and reduced factorial designs. Psychological Methods, 14(3): 202-224. https://doi.org/10.1037/a0015826
[27] Dziak, J.J., Nahum-Shani, I., Collins, L.M. (2012). Multilevel factorial experiments for developing behavioral interventions: Power, sample size, and resource considerations. Psychological Methods, 17(2): 153-175. https://doi.org/10.1037/a0026972
[28] Gunst, R.F., Mason, R.L. (2009). Fractional factorial design. WIREs Computational Statistics, 1(2): 234-244. https://doi.org/10.1002/wics.27
[29] Hoshmand, R. (2018). Design of Experiments for Agriculture and the Natural Sciences (2nd ed.). Chapman and Hall/CRC.
[30] Voelkel, J.G. (2008). Fractional factorial designs. In Encyclopedia of Statistics in Quality and Reliability. https://doi.org/10.1002/9780470061572.eqr007
[31] Toman, B. (1994). Bayes optimal designs for two- and three-level factorial experiments. Journal of the American Statistical Association, 89(427): 937-946. https://doi.org/10.1080/01621459.1994.10476827
[32] Chandra, S., Anderson, V.L., McLean, R.A. (1975). Design of experiments: A realistic approach. Journal of the American Statistical Association, 70(352): 961. https://doi.org/10.2307/2285472
[33] Ryan, T.P. (2004). Planning, construction, and statistical analysis of comparative experiments. Journal of Quality Technology, 36(4): 454-457. https://doi.org/10.1080/00224065.2004.11980292
[34] Zhao, Y. (2022). Split-plot designs with few whole plot factors containing clear effects. Fractal and Fractional, 6(8): 453. https://doi.org/10.3390/fractalfract6080453
[35] Singh, A., Chauhan, C.S. (2022). Factorial designing-An essential tool in pharmaceutical optimization. YMER, 21(7): 519-525. https://doi.org/10.37896/ymer21.07/41
[36] Montgomery, D.C., Runger, G.C. (2010). Applied Statistics and Probability for Engineers. John Wiley & Sons.
[37] ISO 14405-1:2025(en). Geometrical product specifications (GPS) — Dimensional tolerancing — Part 1: Linear sizes. https://www.iso.org/obp/ui/es/#iso:std:iso:14405:-1:ed-3:v1:en.
[38] Software and Documentation. https://aberlink.com/support/software-and-documentation/.

NOMENCLATURE

AM	additive manufacturing
CAD	computer-aided design
FDM	fused deposition modeling
PETG	polyethylene terephthalate glycol-modified
RSM	response surface methodology
°C	degrees Celsius
PET	polyethylene terephthalate
PLA	polylactic Acid
FLEX	flexible filaments
PVA	polyvinyl alcohol, water-soluble filament
PC	polycarbonate filament
PP	polypropylene filament
CPE	chlorinated polyethylene filament
PVB	polyvinyl butyral filament
Mpa	megapascal, 1000000 Pa, 1Pa = N/m^2
CMM	coordinate-measuring machine
ANOVA	analysis of variance
DoE	design of experiment
D	controlled diameter
t	test temperature
S	sequence of the test series
GG	least squares method
GX	minimum described element

GN	maximum inscribed element
Din	inner diameter of the controlled samples
t_b	printer bed temperature
t_n	nozzle temperature
ΔDin	relative change in internal diameter of the controlled samples
Din(n)	nominal value of inner diameter
Din(GG)	inner diameter value obtained by the least squares method
ΔDout	relative change in the outer diameter of the controlled samples
Dout(n)	nominal value of outer diameter
Dout(GG)	outer diameter value obtained by the least squares method
Δt_n	change in nozzle temperature
Δt_b	change in bed temperature
ΔD	relative change in diameter of the controlled samples
D(n)	nominal diameter

Greek symbols

μm	micrometer, $1*10^{-3}$mm
Δ	differance
εδ	relative error in μм/mm

Subscripts

n	nozzle temperature
k	serial number of the test at a step of 5ºC
b	bed temperature
j	sequential number of the experiment in step 5℃